AMERICAN SOCIETY FOR MICROBIOLOGY | mBio®

RESEARCH ARTICLE
Host-Microbe Biology

Streptococcus agalactiae Induces Placental Macrophages To Release Extracellular Traps Loaded with Tissue Remodeling Enzymes via an Oxidative Burst-Dependent Mechanism

Ryan S. Doster,[a] Jessica A. Sutton,[b] Lisa M. Rogers,[a] David M. Aronoff,[a,b,c,d] Jennifer A. Gaddy[a,e]

[a]Division of Infectious Diseases, Department of Medicine, Vanderbilt University Medical Center, Nashville, Tennessee, USA
[b]Department of Microbiology and Immunology, Meharry Medical College, Nashville, Tennessee, USA
[c]Department of Obstetrics and Gynecology, Vanderbilt University Medical Center, Nashville, Tennessee, USA
[d]Department of Pathology, Microbiology and Immunology, Vanderbilt University Medical Center, Nashville, Tennessee, USA
[e]Department of Veterans Affairs, Tennessee Valley Healthcare Systems, Nashville, Tennessee, USA

ABSTRACT *Streptococcus agalactiae*, or group B *Streptococcus* (GBS), is a common perinatal pathogen. GBS colonization of the vaginal mucosa during pregnancy is a risk factor for invasive infection of the fetal membranes (chorioamnionitis) and its consequences such as membrane rupture, preterm labor, stillbirth, and neonatal sepsis. Placental macrophages, or Hofbauer cells, are fetally derived macrophages present within placental and fetal membrane tissues that perform vital functions for fetal and placental development, including supporting angiogenesis, tissue remodeling, and regulation of maternal-fetal tolerance. Although placental macrophages as tissue-resident innate phagocytes are likely to engage invasive bacteria such as GBS, there is limited information regarding how these cells respond to bacterial infection. Here, we demonstrate *in vitro* that placental macrophages release macrophage extracellular traps (METs) in response to bacterial infection. Placental macrophage METs contain proteins, including histones, myeloperoxidase, and neutrophil elastase similar to neutrophil extracellular traps, and are capable of killing GBS cells. MET release from these cells occurs by a process that depends on the production of reactive oxygen species. Placental macrophage METs also contain matrix metalloproteases that are released in response to GBS and could contribute to fetal membrane weakening during infection. MET structures were identified within human fetal membrane tissues infected *ex vivo*, suggesting that placental macrophages release METs in response to bacterial infection during chorioamnionitis.

IMPORTANCE *Streptococcus agalactiae*, also known as group B *Streptococcus* (GBS), is a common pathogen during pregnancy where infection can result in chorioamnionitis, preterm premature rupture of membranes (PPROM), preterm labor, stillbirth, and neonatal sepsis. Mechanisms by which GBS infection results in adverse pregnancy outcomes are still incompletely understood. This study evaluated interactions between GBS and placental macrophages. The data demonstrate that in response to infection, placental macrophages release extracellular traps capable of killing GBS. Additionally, this work establishes that proteins associated with extracellular trap fibers include several matrix metalloproteinases that have been associated with chorioamnionitis. In the context of pregnancy, placental macrophage responses to bacterial infection might have beneficial and adverse consequences, including protective effects against bacterial invasion, but they may also release important mediators of membrane breakdown that could contribute to membrane rupture or preterm labor.

Received 9 October 2018 **Accepted** 15 October 2018 **Published** 20 November 2018

Citation Doster RS, Sutton JA, Rogers LM, Aronoff DM, Gaddy JA. 2018. *Streptococcus agalactiae* induces placental macrophages to release extracellular traps loaded with tissue remodeling enzymes via an oxidative burst-dependent mechanism. mBio 9:e02084-18. https://doi.org/10.1128/mBio.02084-18.

Editor Victor J. Torres, New York University School of Medicine

Address correspondence to Jennifer A. Gaddy, jennifer.a.gaddy@vumc.org.

D.M.A. and J.A.G. contributed equally to this work.

This article is a direct contribution from a Fellow of the American Academy of Microbiology. Solicited external reviewers: Victor Nizet, University of California, San Diego; Philipp Henneke, Centre for Paediatrics and Adolescent Medicine, Medical Centre, University Freiburg.

KEYWORDS *Streptococcus agalactiae*, extracellular traps, group B *Streptococcus*, macrophages, matrix metalloproteinase

Fifteen million cases of preterm birth, or birth before 37 weeks gestation, occur annually worldwide, including 500,000 cases in the United States, conferring an estimated cost of $26.2 billion (1–3). The World Health Organization estimates that preterm birth complications are a leading cause of death among children under 5 years of age, resulting in nearly 1 million deaths in 2015 (4, 5). In addition to loss of child lives, preterm birth increases risk of chronic health conditions, including neurodevelopmental deficits, metabolic syndrome, cardiovascular abnormalities, chronic kidney disease, and chronic respiratory conditions (6, 7).

Streptococcus agalactiae, also known as group B *Streptococcus* (GBS), is a common perinatal pathogen (8). Approximately 10 to 40% of women are colonized with GBS during late pregnancy (9, 10). Rectovaginal GBS carriage is associated with adverse pregnancy outcomes, including stillbirth, preterm labor, chorioamnionitis, and neonatal sepsis (11–13). Because of the burden and severity of GBS-related adverse pregnancy outcomes, the CDC recommends GBS screening late in gestation and antibiotic prophylaxis during labor (14). This strategy has decreased the incidence of early onset neonatal sepsis but misses mothers that deliver preterm before screening is conducted (14). Despite screening and treatment interventions, GBS remains a leading neonatal pathogen (15).

Pregnancy represents a unique immunologic state in which the maternal immune system must dampen its responses against foreign antigens of the semiallogenic fetus while defending the gravid uterus from infection. Excessive inflammation can drive adverse pregnancy events, including loss of pregnancy, preterm birth, intrauterine growth restriction, and preeclampsia (16). Multiple mechanisms exist to support maternal-fetal tolerance, including production of anti-inflammatory cytokines that alter the number and function of immune cells at the maternal-fetal interface (17–19). Unfortunately, infection is a common complication of pregnancy. Bacterial infection of the fetal membranes, known as chorioamnionitis, occurs most often by ascending infection from the vagina (8, 20, 21). During infection, bacterial products are recognized by pathogen recognition receptors, which then stimulate production of proinflammatory cytokines (20, 22, 23). These inflammatory mediators initiate a cascade of events that result in neutrophil infiltration into the fetal membranes, production and release of matrix metalloproteases (MMPs), and cervical contractions which eventually result in membrane rupture and preterm birth (24).

Macrophages represent 20 to 30% of the leukocytes within gestational tissues (25). In particular, fetally derived macrophages, called Hofbauer cells or placental macrophages (PMs), play key roles in placental invasion, angiogenesis, tissue remodeling, and development (26, 27). The inflammatory state of these cells is carefully regulated throughout pregnancy. As the pregnancy progresses, the M2 or anti-inflammatory and tissue remodeling phenotype predominates to supports fetal development (28–31). PMs contribute to immune tolerance by secretion of anti-inflammatory cytokines, which suppress production of proinflammatory cytokines (32–35). Disruption of appropriate macrophage polarization is associated with abnormal pregnancies, including spontaneous abortions, preterm labor, and preeclampsia (28). We sought to understand how bacterial infection alters PM functions and how these responses may contribute to pathological pregnancies. These studies demonstrate that both PMs and a model macrophage cell line, the PMA-differentiated THP-1 macrophage-like cells, release macrophage extracellular traps (METs) in response to bacterial infection in a process that is dependent upon the generation of reactive oxygen species (ROS). METs, reminiscent of neutrophil extracellular traps (NETs), have recently been recognized as structures released by macrophages under a number of conditions, including infection (36). PM METs contain histones, myeloperoxidase, and neutrophil elastase as well as

several MMPs, and MET structures are found within human fetal membranes infected with GBS *ex vivo*.

RESULTS

Placental macrophages release METs in response to GBS. To understand PM responses to GBS at the host-pathogen interface, isolated PMs were infected *ex vivo* with GBS, and cellular interactions were examined using field-gun high-resolution scanning electron microscopy (SEM). At 1 h after infection, fine, reticular structures were noted extending from macrophages, and these structures were less abundant in uninfected samples (Fig. 1A, bottom panels). These structures resembled NETs. Recent reports suggest that macrophages also release fibers composed of DNA and histones, known as METs (36, 37). To determine whether these structures were METs, macrophages were evaluated by scanning laser confocal microscopy after staining with the DNA binding dye SYTOX Green, which demonstrated extracellular structures extending from PMs that were not seen when PMs were treated with DNase I (Fig. 1A, top panels). Cells were then evaluated to assess the degree to which these structures contained proteins previously associated with NETs and METs, including histones, myeloperoxidase, and neutrophil elastase (36, 37). Each of these proteins colocalized to extracellular DNA structures extending from the PMs (Fig. 1B). The staining for MET-associated proteins was specific, as no fluorescent signal was seen when either a secondary conjugated antibody alone or an isotype control secondary conjugated antibody was used to evaluate these structures (see Fig. S1 in the supplemental material). Together, these data suggest that these structures are METs released by PMs. The extent of MET release was then quantified, and PMs cocultured with GBS released significantly more METs than uninfected cells, and DNase I treatment degraded these extracellular structures (Fig. 1C). Additionally, MET release by PMs occurred in a dose-dependent fashion (Fig. S2A), and MET release was not GBS strain or bacterial species specific, as PMs infected with GBS strain GB037, a capsular type V strain, *Escherichia coli*, or heat-killed bacteria resulted in similar MET release (Fig. S3).

One major immunologic function of extracellular traps is the ability to immobilize and kill microorganisms through the locally high concentration of cellular proteins, including histones that have antimicrobial effects (37, 38). In order to investigate the bactericidal activity of PM METs, PMs were cocultured with GBS cells alone or in the presence of DNase I. After 1 h of infection, significantly more bacterial colony-forming units (CFU) were recovered from cocultures treated with DNase I, suggesting that PM METs have bactericidal activity and that eliminating METs with DNase treatment impaired bacterial killing (Fig. 1D). To verify that DNase treatment itself did not result in significant PM cell death, thus decreasing bactericidal ability, PMs were incubated with DNase I for 1 h prior to washing and stimulating PMs with heat-killed GBS for 24 h. PM TNF-α release was used as a marker of macrophage viability and function; there was no difference in TNF-α from supernatants of cells treated with DNase compared to untreated cells (Fig. S2B). Additionally, live-dead bacterial staining of PMs infected with GBS demonstrated dead GBS cells adjacent to MET fibers (Fig. S2C). Together, these data provide evidence that PMs release METs in response to bacteria and that these structures are capable of killing GBS cells.

Extracellular trap formation, or etosis, occurs by a cell death pathway distinct from pyroptosis and apoptosis (39). To investigate whether GBS infection results in different cell death pathways, GBS-infected PMs were assayed for LDH release as a marker of cellular death, TUNEL staining as a marker of apoptosis, and IL-1β release to indicate pyroptosis. After 1 h of GBS infection, supernatants of PMs cocultured with GBS demonstrated an increase in macrophage death, determined by LDH release (Fig. S4A). However, GBS-infected PMs did not exhibit a significant difference in IL-1β release or TUNEL-positive cells compared to uninfected cells treated with vehicle controls at 1 h (Fig. S4B to D).

PMA-differentiated THP-1 macrophage-like cells release METs after direct bacterial contact. Experiments were conducted to determine whether MET responses

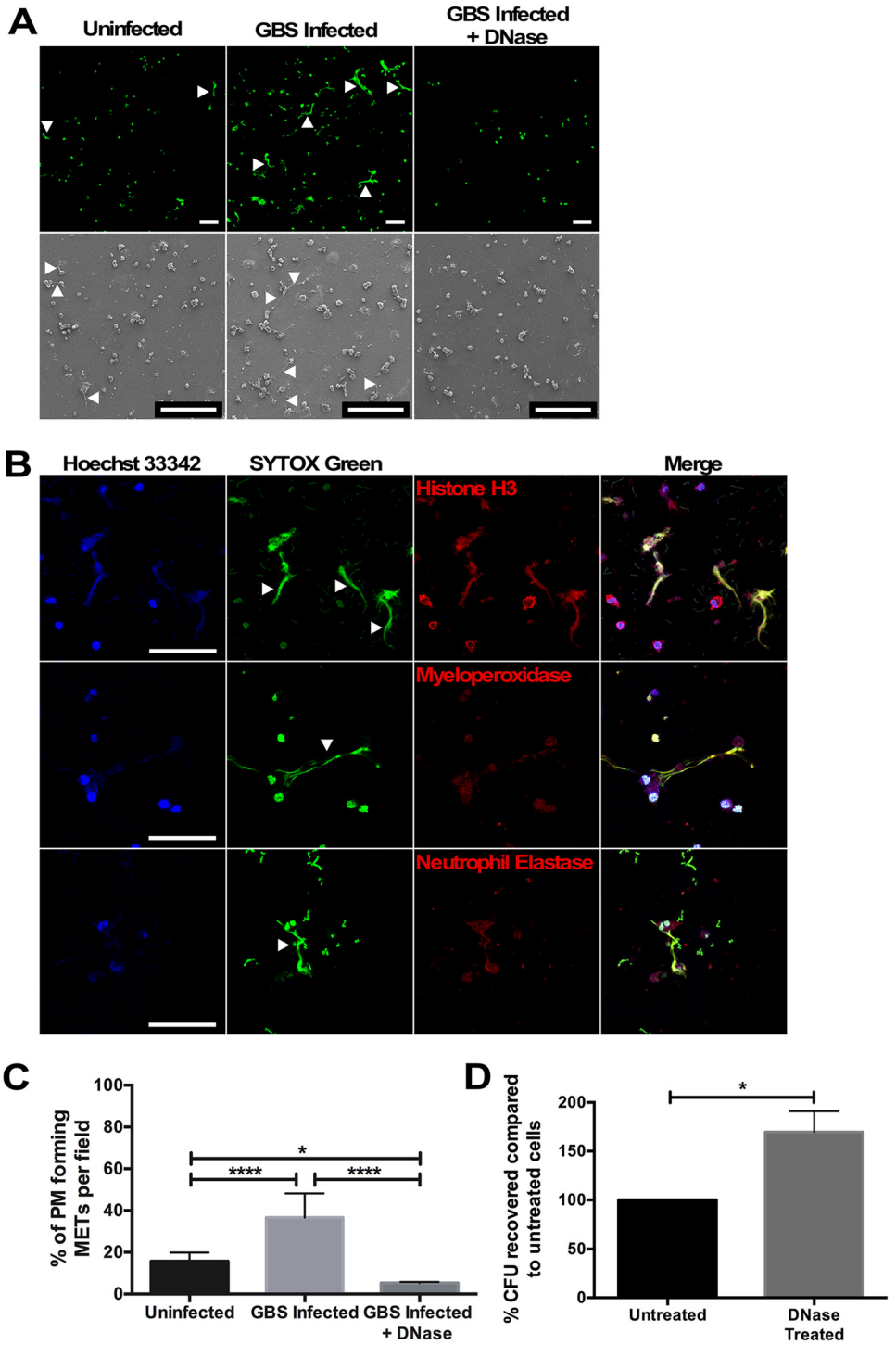

FIG 1 Placental macrophages infected *ex vivo* with GBS-released extracellular traps capable of killing GBS cells. (A) Placental macrophages were infected for 1 h with GBS cells at an MOI of 20:1. Scanning electron micrographs (bottom row) demonstrate extracellular structures released from macrophages (white arrows), which are not seen after DNase I treatment. PMs were also stained with SYTOX Green, a double-stranded DNA dye, and evaluated by scanning laser confocal microscopy, which demonstrates extracellular structures composed of DNA (white arrowheads). Bars represent 100 μm. (B) Placental macrophage extracellular traps were stained with Hoechst 33342 (blue), a condensed chromatin/nuclear stain, SYTOX Green (green), and specific antibodies for either histone H3, myeloperoxidase, or neutrophil elastase as listed (red). Histone, myeloperoxidase, and neutrophil elastase staining colocalizes with extracellular DNA staining, suggesting that MET structures contain these proteins. Bars represent 100 μm. (C) PMs releasing METs were quantified by counting MET-producing cells seen in SEM images and expressed as the number of macrophages releasing METs per field. GBS-infected PMs release significantly more METs than uninfected cells, and DNase I treatment degraded these structures. Data represent samples from 6 to

(Continued on next page)

against GBS were specific to PMs or might represent a broader macrophage response. The immortalized monocyte-like cell line, THP-1 cells, was evaluated after differentiation into macrophage-like cells with phorbol 12-myristate 13-acetate (PMA) for 24 h. THP-1 macrophage-like cells infected with GBS released significantly more METs than uninfected cells, and DNase I treatment degraded the MET structures (Fig. S5). The THP-1 MET response required contact with bacterial cells, as treatment of the macrophage-like cells with sterile filtered bacterial culture supernatant did not stimulate MET release compared to uninfected cells.

Actin polymerization is required for GBS-induced MET release. Actin polymerization has been shown to be important for MET release (36). A similar role of cytoskeletal changes on GBS-induced MET release in THP-1 macrophage-like cells was examined. Treatment prior to infection with the actin polymerization inhibitor, cytochalasin D, but not nocodazole, which inhibits microtubule polymerization, inhibited MET release compared to GBS-infected, untreated cells (Fig. S5). As noted below (and shown in Fig. 2B), cytochalasin D also inhibited MET release by human PMs infected with GBS.

Placental macrophage MET responses require ROS production. Neutrophil release of NETs occurs in a ROS-dependent manner (40). It was hypothesized that MET release from PMs may require production of ROS. Treatment of PMs prior to infection with the NADPH oxidase inhibitor diphenyleneiodonium (DPI) inhibited release of METs, whereas treatment of uninfected macrophages with PMA resulted in similar levels of MET release to GBS-infected cells (Fig. 2A and B). As with the THP-1 macrophage-like cells, treatment of PMs with cytochalasin D prior to infection inhibited MET release. To further define that ROS production was associated with MET release, a fluorescent ROS dye was used to evaluate PMs for intracellular ROS production. Treatment with DPI inhibited ROS production, and GBS infection as well as PMA treatment of uninfected PMs resulted in significantly more ROS production than uninfected cells (Fig. 2C and D). Interestingly, pretreatment with cytochalasin D decreased levels of intracellular ROS production similar to those of DPI, suggesting that pretreatment with the actin cytoskeletal inhibitor may actually be preventing MET release by impeding ROS production. Additionally, ROS production in these experiments mirrored the degree of MET release under similar conditions (Fig. 2B), suggesting that ROS production is necessary for MET release from these macrophages.

Placental macrophage METs contain MMPs. During pregnancy, PMs support gestational tissue remodeling through release of MMPs. Because macrophage release of MMPs has been implicated in the pathogenesis of fetal membrane rupture (41), we hypothesized that these proteases may also be released in METs. Five MMPs that have been implicated in development and pathological pregnancies were evaluated. Immunofluorescent staining of METs was significant for the colocalization of MMP-1, -7, -8, -9, and -12 with extracellular DNA structures (Fig. 3A). As MMPs are present within METs and GBS infection induced MET release, metalloprotease concentrations within coculture supernatants were examined to determine whether GBS infection would result in an increase in metalloprotease release. MMP-8 and MMP-9 have been investigated as potential biomarkers for intrauterine infection (42–44), and concentrations of both were significantly elevated in supernatants of GBS-infected cells compared to uninfected controls (Fig. 3B and C). Global MMP activity of coculture supernatants was then assessed to determine whether the MMPs released were active by using a MMP activity assay, which uses fluorescence resonance energy transfer peptides that, when cleaved

FIG 1 Legend (Continued)
8 different placental samples, one-way ANOVA, $F = 32.7$, $P < 0.0001$, with *post hoc* Tukey's multiple-comparison test. (D) Placental macrophage METs kill GBS cells. PMs were infected for 1 h at an MOI of 20:1 in the presence of DNase I to degrade METs or without DNase (Untreated). Untreated wells were treated with DNase I for the last 10 min of infection to break up DNA complexes prior to serial dilution and plating. DNase I treatment significantly impairs bactericidal activity. Data represent the percent recovered colony-forming units (CFU), normalized to untreated cells from 7 separate experiments from different placenta samples, Student's *t* test, $t = 3.224$, df $= 6$, $P = 0.0180$. ****, $P \leq 0.0001$; *, $P \leq 0.05$.

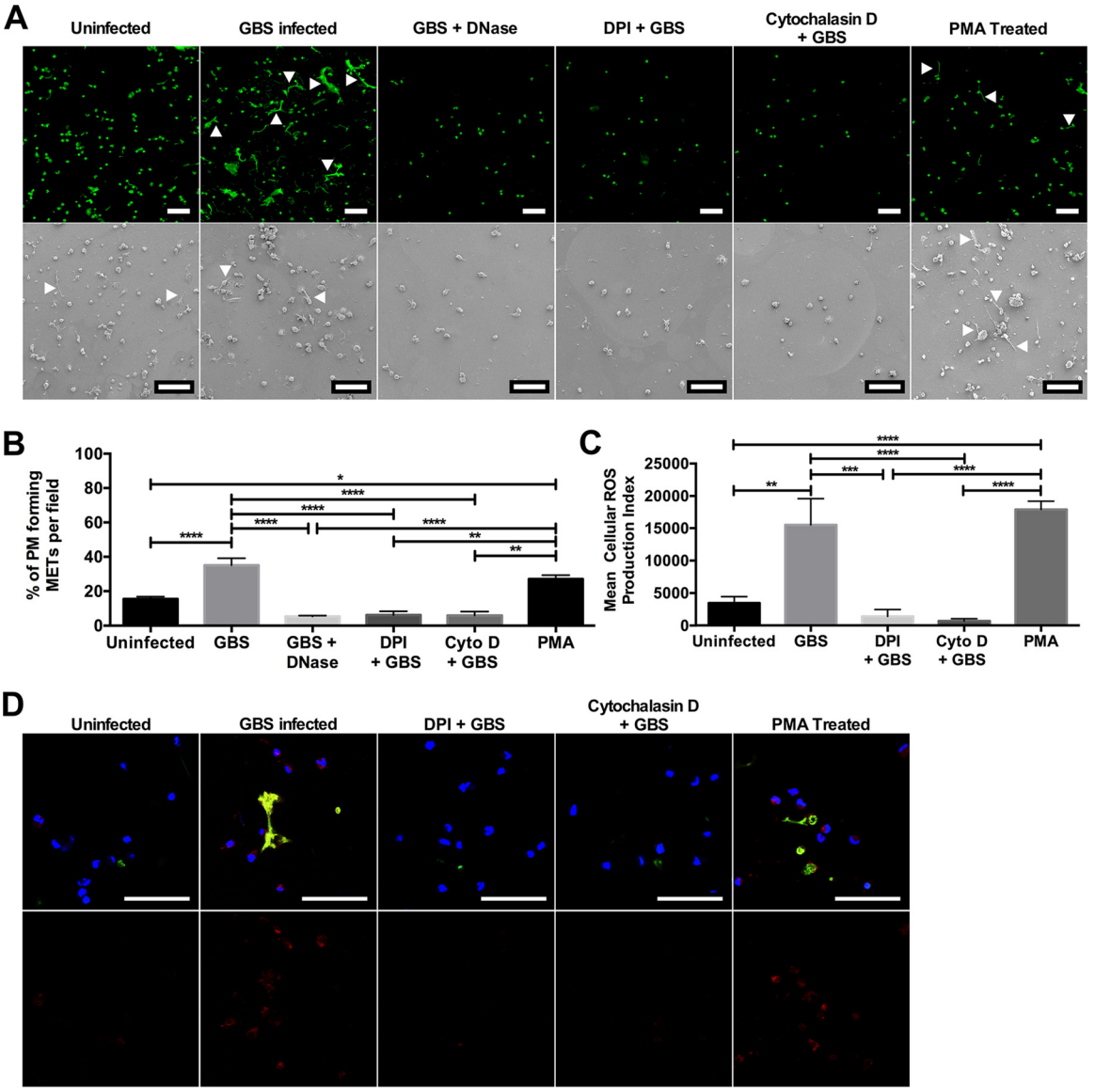

FIG 2 MET release from placental macrophages requires ROS generation. Placental macrophages were incubated with DNase I, DPI to inhibit ROS generation, or cytochalasin D to prevent actin polymerization and then infected with GBS at an MOI of 20:1 for 1 h. Uninfected cells were also stimulated with 500 nM PMA to stimulate protein kinase C activation. (A) Cells were then imaged to identify MET release by confocal microscopy after staining with SYTOX green (top row) or by SEM (bottom row). Bars represent 100 μm. (B) MET release was then quantified as described in the legend to Fig. 1. Treatment with DPI and cytochalasin D significantly inhibited MET release, whereas MET release from PMA-stimulated uninfected cells was not different from GBS-infected cells. Data represent mean ± SE percentage of cells releasing METs per field of 3 to 9 separate experiments, one-way ANOVA, $F = 21.1$, $P < 0.0001$ with Tukey's multiple-comparison test. (C and D) PM cell infections were repeated with staining for intracellular ROS production using CellROX Deep Red reagent. This reagent becomes fluorescent when oxidized by ROS. Cells were cocultured with GBS cells as described above and stained with CellROX Deep Red, SYTOX Green, and Hoechst (top row in panel D). Bars represent 100 μm. ROS production was quantified by measuring the total red fluorescence per image (bottom row in panel D), and the cellular ROS production index was calculated (C). Data are shown from a representative experiment of 3 independent experiments and are expressed as the mean cellular ROS production index plus SE of 10 images from a single placental sample. GBS-infected and PMA-stimulated uninfected cells generated significantly larger amounts of ROS than uninfected cells or those treated with DPI or cytochalasin D (one-way ANOVA, $F = 16.5$, $P < 0.0001$ with *post hoc* Tukey's multiple-comparison test). ****, $P \leq 0.0001$; ***, $P \leq 0.001$; **, $P \leq 0.01$; *, $P \leq 0.05$.

by MMPs, are fluorescent. Supernatants taken from placental macrophages cocultured with GBS demonstrated significantly more MMP activity compared to those of uninfected controls (Fig. 3D). Together, these data suggest that PMs express several MMPs and that these MMPs are released during bacterial infection within METs and into the extracellular spaces, where they might contribute to breakdown of gestational tissue extracellular matrix.

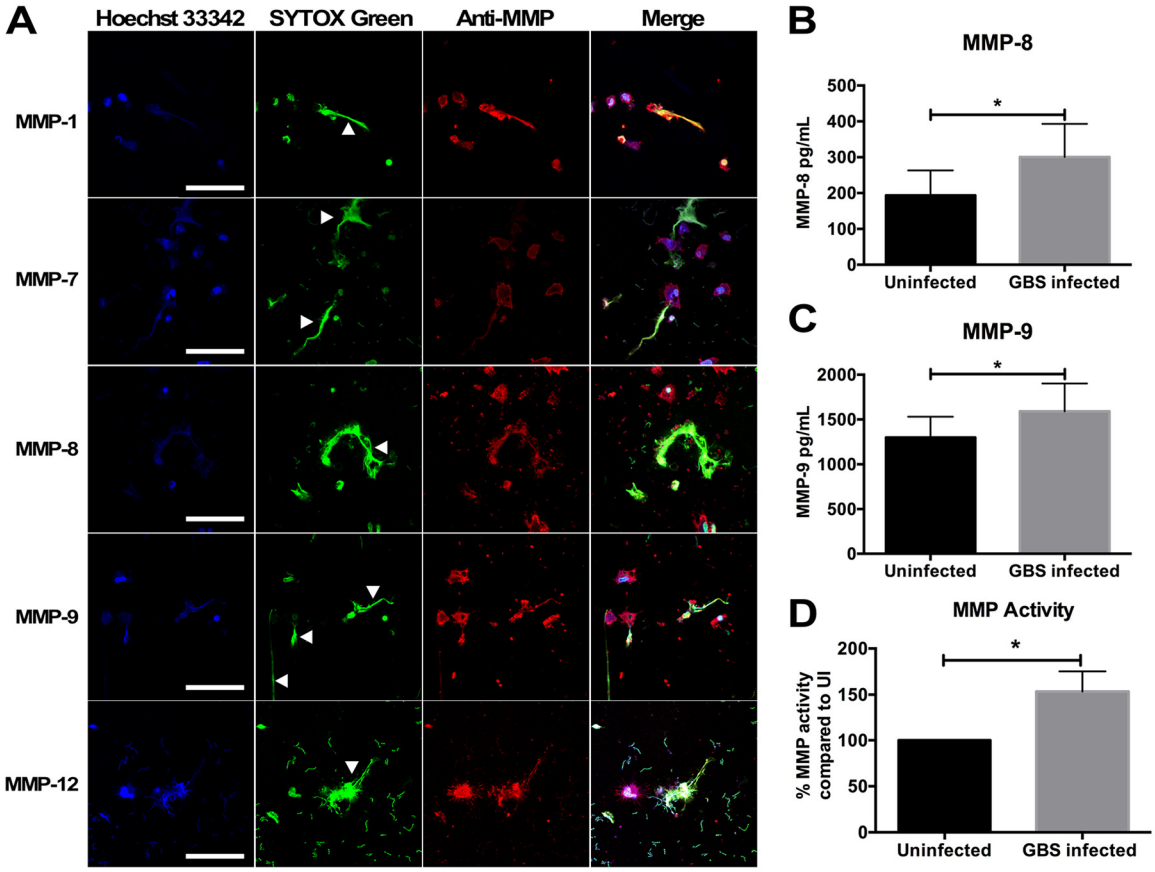

FIG 3 GBS infection results in release of matrix metalloproteinases (MMPs) from placental macrophages. (A) PM METs contain MMP-1, -7, -8, -9, and -12. PMs were infected as described above and then fixed and stained with anti-MMP antibodies and an Alexa Fluor-conjugated secondary antibody (red), Hoechst 33342, and SYTOX green. METs (white arrowheads) stained strongly for MMPs. Bars represent 100 μm. (B and C) Supernatant from PM-GBS cocultures were collected and evaluated for MMP-8 (B) and MMP-9 (C) concentrations by ELISA. GBS infection results in a significant increase in MMP-8 (Student's *t* test, $t = 3.599$, df $= 7$, $P = 0.0087$) and MMP-9 (Student's *t* test, $t = 3.160$, df $= 10$, $P = 0.0102$) release compared to uninfected cells. (D) PMs release active MMPs in response to GBS. Supernatant from PM-GBS coculture was evaluated for MMP activity using a MMP activity assay to assess global MMP activity within coculture supernatants. Supernatant from GBS-infected cells had 53% more MMP activity compared to uninfected PMs (Student's *t* test, $t = 2.439$, df $= 11$, $P = 0.0329$).

MET structures are present in human fetal membrane tissues infected *ex vivo*. To determine whether METs were present within gestational tissues in response to infection, fetal membrane tissues from healthy, term, nonlaboring caesarian sections were obtained, excised, and organized into Transwell structures, creating two chambers separated by the fetal membranes. GBS cells were added to the choriodecidual surface, and infection was allowed to progress for 48 h prior to fixing tissues for immunohistochemistry and immunofluorescence analysis. CD163-positive cells were found localized to an area of GBS microcolonies within the membranes that demonstrated histone staining extending beyond the nucleus and into the extracellular space, suggesting the release of a MET-like structure (Fig. 4A). Immunofluorescence staining demonstrated CD163-positive cells associated with extracellular material that stained positive for histones and MMP-9 (Fig. 4B). Additional staining of fetal membrane tissues using neutrophil elastase as was previously described for identification of NETs in tissues (45), identified cells within the choriodecidua with long extensions that stained strongly for neutrophil elastase that colocalized to histone H3 and DNA staining (Fig. S6). Cells releasing MET-like structures could be compared to cells with intact nuclei and neutrophil elastase staining limited to granule structures, suggesting that cells releasing MET-like structures had undergone cellular changes consistent with etosis.

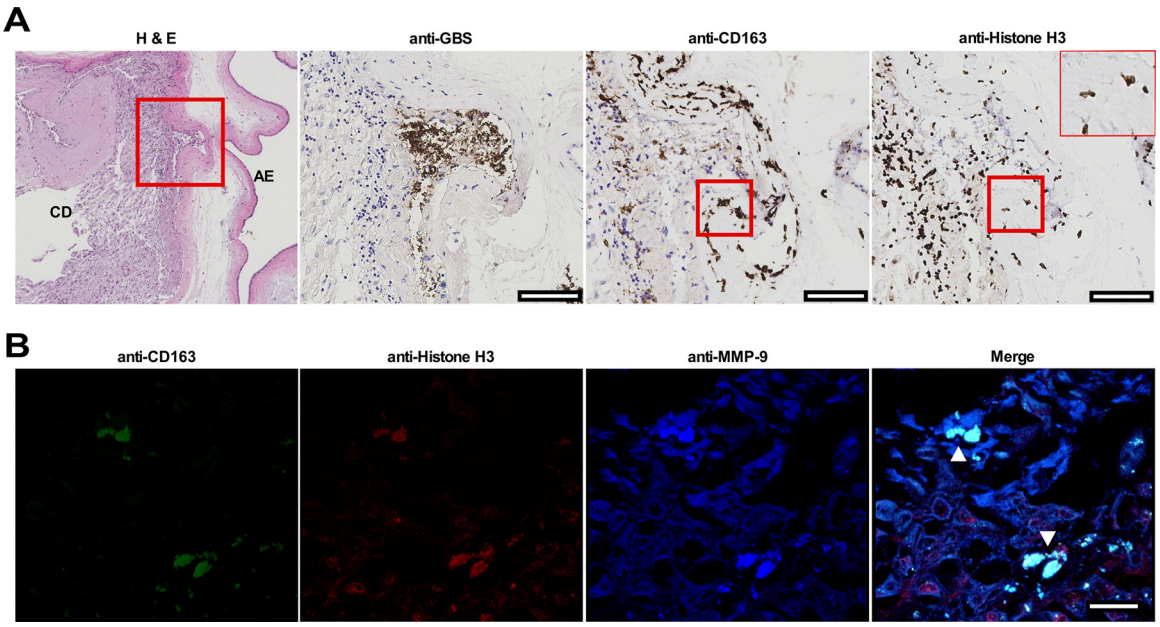

FIG 4 Identification of MET-like structures within human fetal membrane tissues infected with GBS *ex vivo*. Fetal membrane tissues were excised from healthy, term placental tissues from women undergoing routine cesarean section. (A and B) Fetal membrane tissues were then infected with GBS on the choriodecidual surface for 48 h prior to fixation and immunohistochemistry (A) or confocal microscopy (B). (A) Fetal membrane tissues were stained with hematoxylin and eosin (H & E), and representative images are shown at a magnification of ×4. The area within the red box is shown in sections stained with anti-GBS, anti-CD163, or anti-histone H3 antibodies and visualized by immunohistochemistry. GBS cells are able to invade from the choriodecidual surface (CD) toward the amnion epithelium (AE). Macrophages are shown in the area of GBS infection, and macrophages with extracellular histone staining (rightmost image, insert with ×40 magnification) are demonstrated in an area that is also stained with the macrophage marker CD163 (red boxes). Bars represent 100 μm. (B) Fixed and paraffin-embedded fetal membranes were stained with conjugated primary antibodies against CD163, histone H3, and MMP-9. CD163-positive cells within the membrane tissue are seen extruding contents that stain positive for histones and MMP-9 consistent with METs (white arrowheads). Bars represent 20 μm.

DISCUSSION

In the initial description of NETs in 2004, several potential immune functions were described, including the trapping and killing of microorganisms and degradation of bacterial products (37). Release of cellular DNA and proteins within extracellular traps has also been associated with autoimmune pathology in systemic lupus erythematosus and antineutrophil cytoplasmic autoantibodies (ANCA)-associated vasculitis, as well as in diseases of aseptic inflammation (46–50). Other leukocytes, including mast cells, eosinophils, basophils, and macrophages, have now been shown to release extracellular trap structures (36, 51–54).

In this report, PMs are added to a growing list of monocytes and tissue differentiated macrophages capable of releasing METs, which includes human alveolar macrophages, glomerular macrophages, peripheral blood monocytes, and macrophages from other mammalian and nonmammalian species (36). These data demonstrate that human PMs and PMA-differentiated THP-1 macrophage-like cells release METs in response to bacterial infection and after treatment with the protein kinase C agonist, PMA. The present data correlate with previous reports that neutrophils and murine macrophages release traps in response to GBS infection and that METs are capable of killing GBS cells (55, 56).

These data also demonstrate that PM METs contain many proteins previously identified in NETs, including histones, neutrophil elastase, and myeloperoxidase (37). These results mirror other MET investigations demonstrating that diverse macrophages produce and release proteins, including neutrophil elastase within MET structures. For example, human glomerular macrophages releasing METs containing myeloperoxidase have been demonstrated in cases of ANCA-associated glomerulonephritis, and human alveolar macrophages have been shown to release METs containing histones and

MMP-9 (57, 58). Human blood monocytes release METs containing H3 histones, myeloperoxidase, lactoferrin, and neutrophil elastase in response to *Candida albicans* cells, and similar MET contents have been demonstrated in THP-1 macrophage-like cells infected with *Mycobacterium massiliense* (59, 60).

Similar to neutrophil etosis, these data suggest that ROS generation is necessary for PM MET release, as this response was inhibited by treatment with the NADPH oxidase inhibitor DPI. These results mirror reports that inhibition of ROS production via chemical inhibitors resulted in diminished MET release in bovine, caprine, murine, and human macrophages (61–65). In neutrophils, ROS act to break down intracellular membranes and activate neutrophil elastase, which translocates to the nucleus where it degrades histones and promotes chromatin decondensation (39). Myeloperoxidase is thought to contribute chromatin decondensation by an enzyme-independent mechanism (39). It is unclear at this time whether neutrophil elastase and myeloperoxidase perform similar roles in macrophages.

Our data indicate an increase in LDH release during infection, which is consistent with reports that MET release results in cell death (66). Etosis has been noted to be distinct from other cellular death pathways, including pyroptosis and apoptosis. After 1 h of infection when MET responses were identified, there was no significant difference in TUNEL staining or IL-1β release, suggesting that PM METs occur by a distinct pathway. This is notable, as previous reports have shown that the GBS toxin β-hemolysin is capable of inducing pyroptosis of macrophages, though in this study infection was allowed to progress for 4 h, longer than that required for the PM MET response (67). Previous studies have also demonstrated that GBS is capable of inducing macrophage apoptosis, but again this occurred over longer periods of infection than the 1 h that was capable of inducing MET responses (68).

Pretreatment of THP-1 macrophage-like cells and PMs with the actin cytoskeletal inhibitor cytochalasin D inhibited MET release, but not the microtubule inhibitor nocodazole. Conflicting reports exist regarding the role of actin polymerization in etosis. Studies evaluating bovine macrophages and THP-1 cells demonstrated a decrease in MET release after cytochalasin treatment, but similar treatment of murine J744A.1 macrophage-like cells, RAW macrophage-like cells, and bovine blood monocytes did not have a significant effect on MET release (60, 61, 64, 69). This collection of conflicting reports mirrors the NET literature. In the original NET description, cytochalasin D prevented cell phagocytosis but not NET release (37). Others have documented NET inhibition with nocodazole or cytochalasin D in response to LPS or enrofloxacin (70, 71). Because of the differential responses, some authors have postulated that phagocytosis may be an important first step toward cell stimulation and ROS generation, and cytoskeletal inhibition may block the initial steps toward MET release. Another possibility is that the pretreatment with cytochalasin D may interrupt trafficking of the NADPH oxidase complex, thus impairing ROS production. NADPH oxidase is a complex of six components, and the cytosolic proteins $p40^{phox}$ and $p47^{phox}$ are known to interact with F-actin; treatment with cytochalasins have been shown to interrupt NADPH complex formation and lead to impaired ROS formation (72, 73). Timing of the cytochalasin treatment is important, as treatment of cells after prestimulation with molecules such as LPS, which stimulates NADPH oxidase assembly, may actually increase generation of ROS in these cells (74). In our study, macrophages were pretreated with cytochalasin D and were not stimulated prior to infection. It remains unclear whether the conflicting literature with regard to the impact of cytoskeletal inhibition on extracellular traps may be explained by the timing of cytoskeletal inhibition and subsequent effects on ROS production.

PMs were found to produce and release several MMPs within MET structures. During chorioamnionitis, inflammatory mediators lead to the production and release of several metalloproteinases, including MMP-1, MMP-7, MMP-8, and MMP-9 (75, 76). MMP-9 is considered to be the major MMP responsible for collagenase activity within the membranes, but many other MMPs are thought to contribute to the processes of membrane weakening (75, 77). This study reinforces and expands previous reports that

identified placental leukocytes as being able to secrete MMPs, including MMP-1, -7, and -9 (78). Several MMPs have been implicated in preterm birth and pathological pregnancies. MMP-1 and MMP-9 were found to be elevated in placental tissues of women with preterm births compared to women delivering at full term (79). MMP-1 and neutrophil elastase have been shown to stimulate uterine contractions (80). Interestingly, proteomic comparisons of amniotic fluid samples from women with premature preterm rupture of membranes demonstrated increases in histones (H3, H4, and H2B), myeloperoxidase, neutrophil elastase, and MMP-9 in women with histologic chorioamnionitis and proven intrauterine infection, which likely represents the influx of inflammatory cells into these tissues and potentially the release of extracellular traps (81). MMP-12, or macrophage metalloelastase, is a key mediator of the breakdown of elastase and has been shown to be important for spiral artery remodeling during parturition, but to date, there are no studies demonstrating changes in MMP-12 release during cases of pathological pregnancies (82). MMP-12 is better studied in conditions of lung pathology, including emphysema, and alveolar macrophages are known to release MMP-12 in METs during infection, suggesting that protease release from leukocytes may contribute to this disease process (65). Analogous to a controlled burn, we speculate that tethering MMPs to MET structures allows the host to control the release of these potent enzymes, thereby limiting their capacity to broadly weaken membrane structure in response to infection.

MET release appears to occur within fetal membrane tissue, as demonstrated by our immunohistochemistry and immunofluorescence data. This report adds to the growing relevance of these structures in cases of disease pathology. NETs have previously been identified in placenta tissue samples from women with pregnancies complicated by systemic lupus erythematosus and preeclampsia (83, 84). NETs were also found in fetal membrane samples from women with spontaneous preterm labor due to acute chorioamnionitis (85). Interestingly, in this report, antibody staining with histone H3 and neutrophil elastase was used to denote NET structures, but given our data, this staining pattern would not have differentiated METs from NETs. Additionally, our group and others have demonstrated that in animal models of vaginal colonization and perinatal infection with GBS, neutrophils traffic to GBS-infected gestational tissues and release NETs containing antimicrobial peptides, including lactoferrin, as a means to control bacterial growth and invasion (86–88).

In conclusion, we demonstrate that placental macrophages as well as PMA-differentiated THP-1 cells respond to bacterial infection by releasing METs. These MET structures contain proteins similar to those of NETs, including histones, myeloperoxidase, and neutrophil elastase. MET release from these macrophages can be stimulated in the absence of bacterial cells with PMA and is inhibited by pathways that impair ROS production. Placental macrophage METs contain several MMPs that have been implicated in pathological pregnancies, including premature rupture of membranes. MET structures were identified in human fetal membrane tissue infected *ex vivo*. Together, these results suggest that placental macrophages, which are thought to help maintain maternal fetal tolerance and aid in extracellular matrix remodeling, are capable of responding to GBS infection in a way that may trap and kill GBS cells but may also release important mediators of fetal membrane extracellular matrix digestion that could potentially contribute to infection-related pathologies, including preterm rupture of membrane and preterm birth.

MATERIALS AND METHODS

Placental macrophage isolation and culture. Human placental macrophages (PMs) and fetal membrane tissues were isolated from placental tissue samples from women who delivered healthy infants at full term by cesarean section (without labor). Deidentified tissue samples were provided by the Cooperative Human Tissue Network, which is funded by the National Cancer Institute. All tissues were collected in accordance with the guidelines of the Vanderbilt University Institutional Review Board (approval 131607). Macrophage isolation occurred as previously described (89); briefly, placental villous tissue samples were minced followed by digestion with DNase, collagenase, and hyaluronidase (all from Sigma-Aldrich, St. Louis, MO). Cells were filtered and centrifuged, and $CD14^+$ cells were isolated using the magnetic MACS Cell Separation system with CD14 microbeads (Miltenyi Biotec, Auburn, CA). Cells were

incubated in RPMI 1640 medium (ThermoFisher, Waltham, MA) with 10% charcoal stripped fetal bovine serum (ThermoFisher) and 1% antibiotic/antimycotic solution (ThermoFisher) overnight at 37°C in 5% carbon dioxide. The following day, PMs were suspended in RPMI 1640 medium without antibiotic/antimycotic and distributed into polystyrene plates. Cells were incubated for at least 1 h prior to infection to allow for cell adherence to the plate or to poly-L-lysine-coated glass coverslips (Corning, Bedford, MA) for microscopy assays.

THP-1 cell culture. THP-1 cells (ATCC, Manassas VA) were cultured in RPMI 1640 medium with 10% charcoal-treated FBS and 1% antibiotic/antimycotic medium at 37°C in 5% carbon dioxide. Twenty-four to 48 h prior to coculture experiments, cells were treated with 100 nM phorbol 12-myristate 13-acetate (PMA) (Sigma-Aldrich) to induce differentiation to macrophage-like cells. Prior to coculture experiments, cells were suspended in RPMI 1640 medium without antibiotic/antimycotic and distributed into polystyrene plates containing poly-L-lysine-coated glass coverslips and allowed to rest for at least 1 h prior to infection to promote cell adherence.

Bacterial culture. *Streptococcus agalactiae* strain GB590 is a capsular type III, ST-17 strain isolated from a woman with asymptomatic colonization (90), and GB037 is a capsular type V strain obtained from a case of neonatal sepsis (91, 92). *Escherichia coli* serotype 075:H5:K1 is a clinical isolate obtained from a fatal case of neonatal meningitis (93). Bacterial cells were cultured on tryptic soy agar plates supplemented with 5% sheep blood (blood agar plates) at 37°C in ambient air overnight. Bacteria were subcultured from blood agar plates into Todd-Hewitt broth or Luria broth and incubated under aerobic shaking conditions at 37°C in ambient air to stationary phase. Bacterial supernatant was collected and sterile filtered using a 0.1-μm filter (Millipore Sigma, Burlington, MA) and incubated with THP-1 cells at a concentration of 10% volume. Bacterial cells were washed and suspended in phosphate-buffered saline (PBS) (pH 7.4), and bacterial density was measured spectrophotometrically at an optical density of 600 nm (OD_{600}), and bacterial numbers were determined with a coefficient of 1 $OD_{600} = 10^9$ CFU/ml.

Bacterium-macrophage cocultures. PMs or PMA-differentiated macrophage-like cells in RPMI 1640 medium without antibiotics were infected with GBS or *E. coli* cells at a multiplicity of infection (MOI) of 20:1 unless otherwise noted. Cocultured cells were incubated at 37°C in air supplemented with 5% carbon dioxide for 1 h. As stated, some cells were pretreated with 10 μg/ml cytochalasin D (ThermoFisher), 10 nM nocodazole, 100 U/ml DNase I, 500 nM PMA, or 10 μM diphenyleneiodonium chloride (all from Sigma-Aldrich) for at least 20 min prior to infection. At 1 h, supernatants were collected, and cells were fixed with 2.0% paraformaldehyde and 2.5% glutaraldehyde in 0.05 M sodium cacodylate buffer (Electron Microscopy Sciences, Hatfield, PA) for at least 12 h prior to processing for microscopy.

Field-emission gun scanning electron microscopy. After the macrophages were treated and infected as described above, they were incubated in 2.0% paraformaldehyde and 2.5% glutaraldehyde in 0.05 M sodium cacodylate buffer for at least 12 h prior to sequential dehydration with increasing concentrations of ethanol. Samples were dried at the critical point, using a CO_2 drier (Tousimis, Rockville, MD), mounted onto an aluminum stub, and sputter coated with 80/20 gold-palladium. A thin strip of colloidal silver was painted at the sample edge to dissipate sample charging. Samples were imaged with an FEI Quanta 250 field-emission gun scanning electron microscope. Quantification of macrophages producing extracellular traps was determined by evaluating scanning electron micrograph images at a magnification of $\times$750 and counting total macrophages and those macrophages releasing extracellular traps. Extracellular traps were defined as previously described with typical appearing fibers extending from the cell body into the extracellular space (36).

Confocal laser scanning microscopy. Cocultures were completed and macrophages were fixed as described above. Coverslips were washed once with PBS prior to staining with SYTOX Green (final concentration, 10 μM) (ThermoFisher) for double-stranded DNA (dsDNA), and Hoechst 33342 (final concentration, 5 μM) (ThermoFisher) for condensed chromatin (nuclei). Additional staining for histones and MMPs was accomplished by blocking cells in 1% bovine serum albumin in PBS for 30 min at 37°C followed by a 1-h incubation at 37°C with antibodies for histone H3 (ab5103; Abcam, Cambridge, MA), neutrophil elastase (ab68672; Abcam), myeloperoxidase (ab9535; Abcam), matrix metalloproteinase 1 (MMP-1) (ab551168; Abcam), MMP-7 (ab5706; Abcam), MMP-8 (ab81286; Abcam), MMP-9 (ab38898; Abcam), or MMP-12 (ab137444; Abcam). Cells were then washed three times with 1% BSA in PBS, followed by a 30-min incubation with an Alexa Fluor 594-conjugated goat anti-rabbit secondary antibody (ThermoFisher) and two additional washes with 1% BSA in PBS prior to mounting coverslips onto glass microscope slides with Aqua Poly/Mount (Polysciences Inc., Warrington, PA). Macrophages were visualized with a Zeiss LSM 710 META inverted laser scanning confocal microscope, and extracellular traps were identified by dsDNA staining that extended into the extracellular environment.

Bacterial killing by macrophages releasing extracellular traps. PMs were infected with GBS cells at an MOI of 20:1 as described above. As indicated, some PMs were incubated with 100 U/ml DNase I during infection to degrade extracellular trap structures as has been described previously (37). At the end of 1 h, DNase I was added to previously untreated wells for 10 min to release trapped bacterial cells. Supernatants were collected, and PMs were permeabilized with 0.05% Tween 20 in sterile ice-cold water to release intracellular bacteria. Samples were vortexed vigorously, serially diluted, and plated on blood agar plates for enumeration of the bacterial cells. Untreated PMs were compared to DNase I-treated cells, and data are expressed as the percentage of colony-forming units (CFU) recovered compared to that of untreated cells. To further evaluate bacterial killing, PMs were seeded onto coverslips and infected as described above. Following infection, cells were stained using the Live/Dead BacLight bacterial viability kit (Invitrogen) prior to confocal laser scanning microscopy.

LDH cytotoxicity assay. Placental macrophages were incubated in RPMI 1640 medium without antibiotics or serum and infected as described above. Supernatants were collected and centrifuged to

pellet cellular debris. Supernatants were analyzed using the Cytotoxicity Detection kit (Sigma-Aldrich) per the manufacturer's instructions. Results are expressed as percent toxicity using medium without cells as the low control and cells treated with 2% Triton X-100 as the high control. Percent cytotoxicity was calculated using the following equation: cytotoxicity (as a percentage) = (experimental value − low control)/(high control − low control) × 100.

Apoptosis assay. Placental macrophages were incubated in RPMI 1640 medium without antibiotics and infected as described above. Following infection, supernatants were removed, and cells were fixed with 2.0% paraformaldehyde and 2.5% glutaraldehyde in 0.05 M sodium cacodylate buffer for at least 15 min. Click-iT Plus TUNEL assay with Alexa Fluor 594 dye (ThermoFisher) was used to identify cells undergoing apoptosis, and staining was conducted per the manufacturer's instructions with additional staining that included Hoechst 33342 to visualize nuclei prior to confocal laser scanning microscopy.

Macrophage viability assay. To determine whether DNase I treatment resulted in alterations in PM viability or function, TNF-α release was used a functional measure. Cells were left untreated or treated with 100 U/ml DNase I for 60 min. All cells were then washed, and fresh medium was added prior to stimulation with 150:1 heat-killed GBS cells (incubated at 42°C for 2 h) for 24 h. Supernatants were collected and centrifuged to pellet cellular debris before TNF-α release was determined using a DuoSet TNF-α ELISA (R&D Systems) per the manufacturer's instructions.

Measurement of intracellular ROS production. Measurements of intracellular ROS production were made by staining cells with CellRox Deep Red reagent (ThermoFisher) which measures oxidative stress by producing fluorescence upon oxidation by ROS. PMs were isolated and treated as described above. At the time of infection, a cellular stain mixture containing CellROX Deep Red (5 μM final concentration), SYTOX Green, and Hoechst 33342 was added to cocultures. After 1 h of infection, cells were washed three times with PBS before a 15-min fixation with 3.7% formaldehyde to preserve CellRox Reagent signal. Coverslips were then mounted onto glass slides and visualized with a Zeiss LSM 710 confocal microscope as described above. Images obtained were analyzed using Fiji version 1.0 (94). In order to quantify ROS production, a cellular ROS production index was calculated using the following equation: (total image intensity − (mean background fluorescence × image area))/(total macrophages counted × (number of macrophages with ROS production/total macrophages counted)). Images capturing only ROS staining (without other stains/channels) were measured to determine the total corrected fluorescence for the total image area. Mean background fluorescence was determined by at least three different measurements in areas of the image lacking cellular contents (95). Data are presented as the mean ± SE ROS cellular production index of 10 images per sample.

Metalloproteinase ELISA. Supernatants from macrophage-GBS cocultures were collected and centrifuged as described above to remove cellular debris. Supernatants were then evaluated for the concentration of human MMP-8 and MMP-9 using DuoSet ELISA kits (R&D Systems, Minneapolis, MN) per the manufacturer's protocol, and protein levels were calculated from a standard curve.

Matrix metalloproteinase activity. MMP activity of coculture supernatants was measured using the MMP Activity Assay kit (Abcam). Supernatants were incubated with assay buffer for 30 min, and fluorescence signal was measured with a fluorescence microplate reader at an Ex/Em ratio of 490/525 nm. Sample values were normalized to the values for uninfected cells from the same placental sample to calculate percent change for each placental sample assayed.

Human fetal membrane infections. Fetal membrane tissue was obtained and cultured as previously described (96). Briefly, fetal membranes were excised from placental tissues. Fetal membrane tissue sections were suspended over a 12-mm Transwell Permeable Support without membrane (Corning) and immobilized using a 1/4-inch intraoral elastic band (Ormco, Orange, CA) so that the choriodecidua was oriented facing up. Both Transwell chambers were incubated with Dulbecco's modified Eagle's medium (DMEM), high-glucose, HEPES, cell culture medium with no phenol red (Gibco, Carlsbad, California) supplemented with 1% fetal bovine serum and PEN-STREP antibiotic/antimycotic mixture (Gibco). Transwells were incubated overnight at 37°C in ambient air containing 5% CO_2 before the medium was replaced with DMEM, high-glucose, HEPES, cell culture medium with no phenol red (lacking the PEN-STREP antibiotic/antimycotic mixture). Bacterial cells were added to the choriodecidual surface of the gestational membranes at a multiplicity of infection of 1×10^6 cells per Transwell. Cocultures were incubated at 37°C in ambient air containing 5% CO_2 for 48 h at which time membrane tissues were fixed in 10% neutral buffered formalin prior to paraffin embedding.

Human fetal membrane immunohistochemistry staining. Tissues were cut into 5-μm sections, and multiple sections were placed on each slide for analysis. For immunohistochemistry, slides were deparaffinized, and heat-induced antigen retrieval was performed on the Bond Max automated IHC stainer (Leica Biosystems, Buffalo Grove, IL) using their Epitope Retrieval 2 solution for 5 to 20 min. Slides were incubated with a rabbit polyclonal anti-GBS antibody (ab78846; Abcam), rabbit polyclonal anti-histone H3 antibody (ab8580; Abcam), or a mouse monoclonal anti-CD163 antibody (MRQ-26; Cell Marque, Rocklin, CA) for 1 h. The Bond Polymer Refine detection system (Leica Biosystems) was used for visualization. Slides were dehydrated and cleared, and coverslips were added before light microscopy analysis was performed.

Human fetal membrane immunofluorescence staining. For immunofluorescence evaluation of METs within fetal membrane tissue, tissues were fixed and sectioned as described above. Sections were briefly incubated with xylene to deparaffinize. Tissues were blocked for more than 1 h with 10% bovine serum albumin (Sigma-Aldrich) before staining with 1/100 dilutions of mouse monoclonal anti-H3 antibodies conjugated with Alexa Fluor 647 (ab205729; Abcam), rabbit monoclonal anti-CD163 antibodies conjugated with Alexa Fluor 488 (ab218293; Abcam), and mouse monoclonal anti-MMP-9 antibodies conjugated with Alexa Fluor 405 (NBP-259699AF405; Novus Biological, Littleton, CO) overnight at room

temperature. Additional tissue staining was conducted as previously described (45). Tissues were deparaffinized and then incubated in R Universal epitope recovery buffer (Electron Microscopy Sciences, Hatfield, PA) at 50°C for 90 min. Samples were then rinsed in deionized water three times followed by washing with Tris-buffered saline (TBS) (pH 7.4). Samples were permeabilized for 5 min with 0.5% Triton X-100 in TBS at room temperature, followed by three washes with TBS. Samples were then blocked with TBS with 10% BSA for 30 min prior to incubation with 1:50 dilutions of rabbit polyclonal anti-neutrophil elastase antibodies (catalog no. 481001; MilliporeSigma, Burlington, MA) and mouse monoclonal anti-H3 antibodies conjugated with Alexa Fluor 647 in blocking buffer at room temperature overnight. The following day, samples were washed in TBS, followed by repeat blocking with blocking buffer for 30 min at room temperature before incubation with 1/00 dilution of Alexa Fluor 488-conjugated donkey anti-rabbit IgG (Invitrogen) for 4 h at room temperature. Samples were then washed and incubated with 5 μM Hoechst 33342 for 30 min to stain nuclei. After the final washes, slides were dried and coverslips were added to the slides. Tissues were visualized with a Zeiss LSM 710 META inverted laser scanning confocal microscope. Images shown are representative of four separate experiments using tissues from different placental samples.

Statistics. Statistical analysis of MET quantifications was performed using one-way ANOVA with either Tukey's or Dunnet's *post hoc* correction for multiple comparisons, and all reported *P* values are adjusted to account for multiple comparisons. MMP activity assays and bacterial killing assay were normalized to untreated or uninfected cells and analyzed with Student's *t* test or one-way ANOVA. *P* values of $\leq$0.05 were considered significant. All data analyzed in this work were derived from at least three biological replicates (representing different placental samples). Statistical analyses were performed using GraphPad Prism 6 for MAC OS X Software (version 6.0g; GraphPad Software Inc., La Jolla, CA).

SUPPLEMENTAL MATERIAL

Supplemental material for this article may be found at https://doi.org/10.1128/mBio.02084-18.

FIG S1, JPG file, 0.04 MB.
FIG S2, TIF file, 1.1 MB.
FIG S3, JPG file, 0.1 MB.
FIG S4, TIF file, 1.4 MB.
FIG S5, JPG file, 0.1 MB.
FIG S6, TIF file, 1.4 MB.

ACKNOWLEDGMENTS

We thank Oscar Gomez-Duarte and Shannon Manning for providing the clinical bacterial isolates used in this study.

Core services, including use of the Cell Imaging Shared Resource, were performed through support from the Vanderbilt Institute for Clinical and Translational Research program supported by the National Center for Research Resources (grant UL1 RR024975-01) and the National Center for Advancing Translational Sciences (grant 2 UL1 TR000445-06). Deidentified, human fetal membrane tissue samples were provided by the Cooperative Human Tissue Network at Vanderbilt University, which is funded by the National Cancer Institute.

The funders of this study had no role in study design, data collection and interpretation, or the decision to submit the work for publication.

We have no conflicts of interest to disclose.

REFERENCES

1. Blencowe H, Cousens S, Chou D, Oestergaard M, Say L, Moller AB, Kinney M, Lawn J, Born Too Soon Preterm Birth Action Group. 2013. Born too soon: the global epidemiology of 15 million preterm births. Reprod Health 10(Suppl 1):S2. https://doi.org/10.1186/1742-4755-10-S1-S2.
2. March of Dimes. October 2013. The impact of premature birth on society. Prematurity Campaign. March of Dimes, White Plains, NY. http://www.marchofdimes.org/mission/the-economic-and-societal-costs.aspx. Accessed 21 January 2015.
3. World Health Organization. 2012. Born too soon: the global action report on preterm birth. World Health Organization, Geneva, Switzerland.
4. World Health Organization. 2016. Fact sheet on preterm birth. World Health Organization, Geneva, Switzerland. http://www.who.int/mediacentre/factsheets/fs363/en/. Accessed 26 September 2017.
5. Liu L, Oza S, Hogan D, Chu Y, Perin J, Zhu J, Lawn JE, Cousens S, Mathers C, Black RE. 2016. Global, regional, and national causes of under-5 mortality in 2000-15: an updated systematic analysis with implications for the Sustainable Development Goals. Lancet 388:3027–3035. https://doi.org/10.1016/S0140-6736(16)31593-8.
6. Luu TM, Rehman Mian MO, Nuyt AM. 2017. Long-term impact of preterm birth: neurodevelopmental and physical health outcomes. Clin Perinatol 44:305–314. https://doi.org/10.1016/j.clp.2017.01.003.
7. Doyle LW. 2008. Cardiopulmonary outcomes of extreme prematurity. Semin Perinatol 32:28–34. https://doi.org/10.1053/j.semperi.2007.12.005.
8. Mendz GL, Kaakoush NO, Quinlivan JA. 2013. Bacterial aetiological agents of intra-amniotic infections and preterm birth in pregnant women. Front Cell Infect Microbiol 3:58. https://doi.org/10.3389/fcimb.2013.00058.
9. Kwatra G, Adrian PV, Shiri T, Buchmann EJ, Cutland CL, Madhi SA. 2014. Serotype-specific acquisition and loss of group B streptococcus recto-

vaginal colonization in late pregnancy. PLoS One 9:e98778. https://doi.org/10.1371/journal.pone.0098778.
10. Russell NJ, Seale AC, O'Driscoll M, O'Sullivan C, Bianchi-Jassir F, Gonzalez-Guarin J, Lawn JE, Baker CJ, Bartlett L, Cutland C, Gravett MG, Heath PT, Le Doare K, Madhi SA, Rubens CE, Schrag S, Sobanjo-Ter Meulen A, Vekemans J, Saha SK, Ip M, GBS Maternal Colonization Investigator Group. 2017. Maternal colonization with group B Streptococcus and serotype distribution worldwide: systematic review and meta-analyses. Clin Infect Dis 65:S100–S111. https://doi.org/10.1093/cid/cix658.
11. Benitz WE, Gould JB, Druzin ML. 1999. Risk factors for early-onset group B streptococcal sepsis: estimation of odds ratios by critical literature review. Pediatrics 103:e77. https://doi.org/10.1542/peds.103.6.e77.
12. Seale AC, Blencowe H, Bianchi-Jassir F, Embleton N, Bassat Q, Ordi J, Menendez C, Cutland C, Briner C, Berkley JA, Lawn JE, Baker CJ, Bartlett L, Gravett MG, Heath PT, Ip M, Le Doare K, Rubens CE, Saha SK, Schrag S, Meulen AS, Vekemans J, Madhi SA. 2017. Stillbirth with group B Streptococcus disease worldwide: systematic review and meta-analyses. Clin Infect Dis 65:S125–S132. https://doi.org/10.1093/cid/cix585.
13. Bianchi-Jassir F, Seale AC, Kohli-Lynch M, Lawn JE, Baker CJ, Bartlett L, Cutland C, Gravett MG, Heath PT, Ip M, Le Doare K, Madhi SA, Saha SK, Schrag S, Sobanjo-Ter Meulen A, Vekemans J, Rubens CE. 2017. Preterm birth associated with group B Streptococcus maternal colonization worldwide: systematic review and meta-analyses. Clin Infect Dis 65: S133–S142. https://doi.org/10.1093/cid/cix661.
14. Verani JR, McGee L, Schrag SJ, Division of Bacterial Diseases, National Center for Immunization and Respiratory Diseases, Centers for Disease Control and Prevention (CDC). 2010. Prevention of perinatal group B streptococcal disease–revised guidelines from CDC, 2010. MMWR Recomm Rep 59:1–36.
15. Stoll BJ, Hansen NI, Sánchez PJ, Faix RG, Poindexter BB, Van Meurs KP, Bizzarro MJ, Goldberg RN, Frantz ID, III, Hale EC, Shankaran S, Kennedy K, Carlo WA, Watterberg KL, Bell EF, Walsh MC, Schibler K, Laptook AR, Shane AL, Schrag SJ, Das A, Higgins RD, Eunice Kennedy Shriver National Institute of Child Health and Human Development Neonatal Research Network. 2011. Early onset neonatal sepsis: the burden of group B streptococcal and E. coli disease continues. Pediatrics 127:817–826. https://doi.org/10.1542/peds.2010-2217.
16. Ghaebi M, Nouri M, Ghasemzadeh A, Farzadi L, Jadidi-Niaragh F, Ahmadi M, Yousefi M. 2017. Immune regulatory network in successful pregnancy and reproductive failures. Biomed Pharmacother 88:61–73. https://doi.org/10.1016/j.biopha.2017.01.016.
17. Arck PC, Hecher K. 2013. Fetomaternal immune cross-talk and its consequences for maternal and offspring's health. Nat Med 19:548–556. https://doi.org/10.1038/nm.3160.
18. Xu YY, Wang SC, Li DJ, Du MR. 2017. Co-signaling molecules in maternal-fetal immunity. Trends Mol Med 23:46–58. https://doi.org/10.1016/j.molmed.2016.11.001.
19. Nagamatsu T, Barrier BF, Schust DJ. 2011. The regulation of T-cell cytokine production by ICOS-B7H2 interactions at the human fetomaternal interface. Immunol Cell Biol 89:417–425. https://doi.org/10.1038/icb.2010.101.
20. Goldenberg RL, Hauth JC, Andrews WW. 2000. Intrauterine infection and preterm delivery. N Engl J Med 342:1500–1507. https://doi.org/10.1056/NEJM200005183422007.
21. Kim CJ, Romero R, Chaemsaithong P, Chaiyasit N, Yoon BH, Kim YM. 2015. Acute chorioamnionitis and funisitis: definition, pathologic features, and clinical significance. Am J Obstet Gynecol 213:S29–S52. https://doi.org/10.1016/j.ajog.2015.08.040.
22. Anders AP, Gaddy JA, Doster RS, Aronoff DM. 2017. Current concepts in maternal-fetal immunology: recognition and response to microbial pathogens by decidual stromal cells. Am J Reprod Immunol 77:e12623. https://doi.org/10.1111/aji.12623.
23. Stallmach T, Hebisch G, Joller H, Kolditz P, Engelmann M. 1995. Expression pattern of cytokines in the different compartments of the feto-maternal unit under various conditions. Reprod Fertil Dev 7:1573–1580. https://doi.org/10.1071/RD9951573.
24. Agrawal V, Hirsch E. 2012. Intrauterine infection and preterm labor. Semin Fetal Neonatal Med 17:12–19. https://doi.org/10.1016/j.siny.2011.09.001.
25. Houser BL. 2012. Decidual macrophages and their roles at the maternal-fetal interface. Yale J Biol Med 85:105–118.
26. Reyes L, Wolfe B, Golos T. 2017. Hofbauer cells: placental macrophages of fetal origin. Results Probl Cell Differ 62:45–60. https://doi.org/10.1007/978-3-319-54090-0_3.
27. Brown MB, von Chamier M, Allam AB, Reyes L. 2014. M1/M2 macrophage polarity in normal and complicated pregnancy. Front Immunol 5:606. https://doi.org/10.3389/fimmu.2014.00606.
28. Zhang YH, He M, Wang Y, Liao AH. 2017. Modulators of the balance between M1 and M2 macrophages during pregnancy. Front Immunol 8:120. https://doi.org/10.3389/fimmu.2017.00120.
29. Mantovani A, Biswas SK, Galdiero MR, Sica A, Locati M. 2013. Macrophage plasticity and polarization in tissue repair and remodelling. J Pathol 229:176–185. https://doi.org/10.1002/path.4133.
30. Kim SY, Romero R, Tarca AL, Bhatti G, Kim CJ, Lee J, Elsey A, Than NG, Chaiworapongsa T, Hassan SS, Kang GH, Kim JS. 2012. Methylome of fetal and maternal monocytes and macrophages at the feto-maternal interface. Am J Reprod Immunol 68:8–27. https://doi.org/10.1111/j.1600-0897.2012.01108.x.
31. Gustafsson C, Mjosberg J, Matussek A, Geffers R, Matthiesen L, Berg G, Sharma S, Buer J, Ernerudh J. 2008. Gene expression profiling of human decidual macrophages: evidence for immunosuppressive phenotype. PLoS One 3:e2078. https://doi.org/10.1371/journal.pone.0002078.
32. Johnson EL, Chakraborty R. 2012. Placental Hofbauer cells limit HIV-1 replication and potentially offset mother to child transmission (MTCT) by induction of immunoregulatory cytokines. Retrovirology 9:101. https://doi.org/10.1186/1742-4690-9-101.
33. Chen CP, Tsai PS, Huang CJ. 2012. Antiinflammation effect of human placental multipotent mesenchymal stromal cells is mediated by prostaglandin E2 via a myeloid differentiation primary response gene 88-dependent pathway. Anesthesiology 117:568–579. https://doi.org/10.1097/ALN.0b013e31826150a9.
34. Montero J, Gomez-Abellan V, Arizcun M, Mulero V, Sepulcre MP. 2016. Prostaglandin E2 promotes M2 polarization of macrophages via a cAMP/CREB signaling pathway and deactivates granulocytes in teleost fish. Fish Shellfish Immunol 55:632–641. https://doi.org/10.1016/j.fsi.2016.06.044.
35. Wetzka B, Clark DE, Charnock-Jones DS, Zahradnik HP, Smith SK. 1997. Isolation of macrophages (Hofbauer cells) from human term placenta and their prostaglandin E2 and thromboxane production. Hum Reprod 12:847–852. https://doi.org/10.1093/humrep/12.4.847.
36. Doster RS, Rogers LM, Gaddy JA, Aronoff DM. 2018. Macrophage extracellular traps: a scoping review. J Innate Immun 10:3–13. https://doi.org/10.1159/000480373.
37. Brinkmann V, Reichard U, Goosmann C, Fauler B, Uhlemann Y, Weiss DS, Weinrauch Y, Zychlinsky A. 2004. Neutrophil extracellular traps kill bacteria. Science 303:1532–1535. https://doi.org/10.1126/science.1092385.
38. Hirsch JG. 1958. Bactericidal action of histone. J Exp Med 108:925–944. https://doi.org/10.1084/jem.108.6.925.
39. Papayannopoulos V, Metzler KD, Hakkim A, Zychlinsky A. 2010. Neutrophil elastase and myeloperoxidase regulate the formation of neutrophil extracellular traps. J Cell Physiol 191:677–691. https://doi.org/10.1083/jcb.201006052.
40. Stoiber W, Obermayer A, Steinbacher P, Krautgartner WD. 2015. The role of reactive oxygen species (ROS) in the formation of extracellular traps (ETs) in humans. Biomolecules 5:702–723. https://doi.org/10.3390/biom5020702.
41. Gomez-Lopez N, StLouis D, Lehr MA, Sanchez-Rodriguez EN, Arenas-Hernandez M. 2014. Immune cells in term and preterm labor. Cell Mol Immunol 11:571–581. https://doi.org/10.1038/cmi.2014.46.
42. Chaemsaithong P, Romero R, Docheva N, Chaiyasit N, Bhatti G, Pacora P, Hassan SS, Yeo L, Erez O. 2018. Comparison of rapid MMP-8 and interleukin-6 point-of-care tests to identify intra-amniotic inflammation/infection and impending preterm delivery in patients with preterm labor and intact membranes. J Matern Fetal Neonatal Med 31:228–244. https://doi.org/10.1080/14767058.2017.1281904.
43. Kim KW, Romero R, Park HS, Park CW, Shim SS, Jun JK, Yoon BH. 2007. A rapid matrix metalloproteinase-8 bedside test for the detection of intra-amniotic inflammation in women with preterm premature rupture of membranes. Am J Obstet Gynecol 197:292.e1–292.e5. https://doi.org/10.1016/j.ajog.2007.06.040.
44. Angus SR, Segel SY, Hsu CD, Locksmith GJ, Clark P, Sammel MD, Macones GA, Strauss JF, III, Parry S. 2001. Amniotic fluid matrix metalloproteinase-8 indicates intra-amniotic infection. Am J Obstet Gynecol 185:1232–1238. https://doi.org/10.1067/mob.2001.118654.
45. Brinkmann V, Abu Abed U, Goosmann C, Zychlinsky A. 2016. Immunodetection of NETs in paraffin-embedded tissue. Front Immunol 7:513. https://doi.org/10.3389/fimmu.2016.00513.
46. Simon D, Simon HU, Yousefi S. 2013. Extracellular DNA traps in allergic,

infectious, and autoimmune diseases. Allergy 68:409–416. https://doi.org/10.1111/all.12111.
47. Soderberg D, Segelmark M. 2016. Neutrophil extracellular traps in ANCA-associated vasculitis. Front Immunol 7:256. https://doi.org/10.3389/fimmu.2016.00256.
48. Delgado-Rizo V, Martínez-Guzmán MA, Iñiguez-Gutierrez L, García-Orozco A, Alvarado-Navarro A, Fafutis-Morris M. 2017. Neutrophil extracellular traps and its implications in inflammation: an overview. Front Immunol 8:81. https://doi.org/10.3389/fimmu.2017.00081.
49. Fuchs TA, Brill A, Duerschmied D, Schatzberg D, Monestier M, Myers DD, Jr, Wrobleski SK, Wakefield TW, Hartwig JH, Wagner DD. 2010. Extracellular DNA traps promote thrombosis. Proc Natl Acad Sci U S A 107:15880–15885. https://doi.org/10.1073/pnas.1005743107.
50. Schorn C, Janko C, Krenn V, Zhao Y, Munoz LE, Schett G, Herrmann M. 2012. Bonding the foe - NETting neutrophils immobilize the pro-inflammatory monosodium urate crystals. Front Immunol 3:376. https://doi.org/10.3389/fimmu.2012.00376.
51. Mollerherm H, von Kockritz-Blickwede M, Branitzki-Heinemann K. 2016. Antimicrobial activity of mast cells: role and relevance of extracellular DNA traps. Front Immunol 7:265. https://doi.org/10.3389/fimmu.2016.00265.
52. Yousefi S, Gold JA, Andina N, Lee JJ, Kelly AM, Kozlowski E, Schmid I, Straumann A, Reichenbach J, Gleich GJ, Simon HU. 2008. Catapult-like release of mitochondrial DNA by eosinophils contributes to antibacterial defense. Nat Med 14:949–953. https://doi.org/10.1038/nm.1855.
53. Morshed M, Hlushchuk R, Simon D, Walls AF, Obata-Ninomiya K, Karasuyama H, Djonov V, Eggel A, Kaufmann T, Simon HU, Yousefi S. 2014. NADPH oxidase-independent formation of extracellular DNA traps by basophils. J Immunol 192:5314–5323. https://doi.org/10.4049/jimmunol.1303418.
54. von Kockritz-Blickwede M, Goldmann O, Thulin P, Heinemann K, Norrby-Teglund A, Rohde M, Medina E. 2008. Phagocytosis-independent antimicrobial activity of mast cells by means of extracellular trap formation. Blood 111:3070–3080. https://doi.org/10.1182/blood-2007-07-104018.
55. Vega VL, Crotty Alexander LE, Charles W, Hwang JH, Nizet V, De Maio A. 2014. Activation of the stress response in macrophages alters the M1/M2 balance by enhancing bacterial killing and IL-10 expression. J Mol Med (Berl) 92:1305–1317. https://doi.org/10.1007/s00109-014-1201-y.
56. Carlin AF, Uchiyama S, Chang YC, Lewis AL, Nizet V, Varki A. 2009. Molecular mimicry of host sialylated glycans allows a bacterial pathogen to engage neutrophil Siglec-9 and dampen the innate immune response. Blood 113:3333–3336. https://doi.org/10.1182/blood-2008-11-187302.
57. O'Sullivan KM, Lo CY, Summers SA, Elgass KD, McMillan PJ, Longano A, Ford SL, Gan P-Y, Kerr PG, Richard Kitching A, Holdsworth SR. 2015. Renal participation of myeloperoxidase in antineutrophil cytoplasmic antibody (ANCA)-associated glomerulonephritis. Kidney Int 88:1030–1046. https://doi.org/10.1038/ki.2015.202.
58. Sharma R, O'Sullivan KM, Holdsworth SR, Bardin PG, King PT. 2017. Visualizing macrophage extracellular traps using confocal microscopy. J Vis Exp [. https://doi.org/10.3791/56459.
59. Halder LD, Abdelfatah MA, Jo EA, Jacobsen ID, Westermann M, Beyersdorf N, Lorkowski S, Zipfel PF, Skerka C. 2016. Factor H binds to extracellular DNA traps released from human blood monocytes in response to Candida albicans. Front Immunol 7:671. https://doi.org/10.3389/fimmu.2016.00671.
60. Je S, Quan H, Yoon Y, Na Y, Kim BJ, Seok SH. 2016. Mycobacterium massiliense induces macrophage extracellular traps with facilitating bacterial growth. PLoS One 11:e0155685. https://doi.org/10.1371/journal.pone.0155685.
61. Aulik NA, Hellenbrand KM, Czuprynski CJ. 2012. Mannheimia haemolytica and its leukotoxin cause macrophage extracellular trap formation by bovine macrophages. Infect Immun 80:1923–1933. https://doi.org/10.1128/IAI.06120-11.
62. Hellenbrand KM, Forsythe KM, Rivera-Rivas JJ, Czuprynski CJ, Aulik NA. 2013. Histophilus somni causes extracellular trap formation by bovine neutrophils and macrophages. Microb Pathog 54:67–75. https://doi.org/10.1016/j.micpath.2012.09.007.
63. Perez D, Munoz MC, Molina JM, Munoz-Caro T, Silva LM, Taubert A, Hermosilla C, Ruiz A. 2016. Eimeria ninakohlyakimovae induces NADPH oxidase-dependent monocyte extracellular trap formation and upregulates IL-12 and TNF-alpha, IL-6 and CCL2 gene transcription. Vet Parasitol 227:143–150. https://doi.org/10.1016/j.vetpar.2016.07.028.
64. Munoz-Caro T, Silva LM, Ritter C, Taubert A, Hermosilla C. 2014. Besnoitia besnoiti tachyzoites induce monocyte extracellular trap formation. Parasitol Res 113:4189–4197. https://doi.org/10.1007/s00436-014-4094-3.
65. King PT, Sharma R, O'Sullivan K, Selemidis S, Lim S, Radhakrishna N, Lo C, Prasad J, Callaghan J, McLaughlin P, Farmer M, Steinfort D, Jennings B, Ngui J, Broughton BR, Thomas B, Essilfie AT, Hickey M, Holmes PW, Hansbro P, Bardin PG, Holdsworth SR. 2015. Nontypeable Haemophilus influenzae induces sustained lung oxidative stress and protease expression. PLoS One 10:e0120371. https://doi.org/10.1371/journal.pone.0120371.
66. Chow OA, von Kockritz-Blickwede M, Bright AT, Hensler ME, Zinkernagel AS, Cogen AL, Gallo RL, Monestier M, Wang Y, Glass CK, Nizet V. 2010. Statins enhance formation of phagocyte extracellular traps. Cell Host Microbe 8:445–454. https://doi.org/10.1016/j.chom.2010.10.005.
67. Whidbey C, Vornhagen J, Gendrin C, Boldenow E, Samson JM, Doering K, Ngo L, Ezekwe EA, Jr, Gundlach JH, Elovitz MA, Liggitt D, Duncan JA, Adams Waldorf KM, Rajagopal L. 2015. A streptococcal lipid toxin induces membrane permeabilization and pyroptosis leading to fetal injury. EMBO Mol Med 7:488–505. https://doi.org/10.15252/emmm.201404883.
68. Fettucciari K, Rosati E, Scaringi L, Cornacchione P, Migliorati G, Sabatini R, Fetriconi I, Rossi R, Marconi P. 2000. Group B Streptococcus induces apoptosis in macrophages. J Immunol 165:3923–3933. https://doi.org/10.4049/jimmunol.165.7.3923.
69. Liu P, Wu X, Liao C, Liu X, Du J, Shi H, Wang X, Bai X, Peng P, Yu L, Wang F, Zhao Y, Liu M. 2014. Escherichia coli and Candida albicans induced macrophage extracellular trap-like structures with limited microbicidal activity. PLoS One 9:e90042. https://doi.org/10.1371/journal.pone.0090042.
70. Jerjomiceva N, Seri H, Vollger L, Wang Y, Zeitouni N, Naim HY, von Kockritz-Blickwede M. 2014. Enrofloxacin enhances the formation of neutrophil extracellular traps in bovine granulocytes. J Innate Immun 6:706–712. https://doi.org/10.1159/000358881.
71. Neeli I, Dwivedi N, Khan S, Radic M. 2009. Regulation of extracellular chromatin release from neutrophils. J Innate Immun 1:194–201. https://doi.org/10.1159/000206974.
72. Touyz RM, Yao G, Quinn MT, Pagano PJ, Schiffrin EL. 2005. p47phox associates with the cytoskeleton through cortactin in human vascular smooth muscle cells: role in NAD(P)H oxidase regulation by angiotensin II. Arterioscler Thromb Vasc Biol 25:512–518. https://doi.org/10.1161/01.ATV.0000154141.66879.98.
73. Shao D, Segal AW, Dekker LV. 2010. Subcellular localisation of the p40phox component of NADPH oxidase involves direct interactions between the Phox homology domain and F-actin. Int J Biochem Cell Biol 42:1736–1743. https://doi.org/10.1016/j.biocel.2010.07.009.
74. Voloshina EV, Prasol EA, Grachev SV, Prokhorenko IR. 2009. Effect of cytochalasin D on the respiratory burst of primed neutrophils activated with a secondary stimulus. Dokl Biochem Biophys 424:13–15. https://doi.org/10.1134/S1607672909010049.
75. Weiss A, Goldman S, Shalev E. 2007. The matrix metalloproteinases (MMPS) in the decidua and fetal membranes. Front Biosci 12:649–659. https://doi.org/10.2741/2089.
76. Nishihara S, Someya A, Yonemoto H, Ota A, Itoh S, Nagaoka I, Takeda S. 2008. Evaluation of the expression and enzyme activity of matrix metalloproteinase-7 in fetal membranes during premature rupture of membranes at term in humans. Reprod Sci 15:156–165. https://doi.org/10.1177/1933719107310308.
77. Kumar D, Moore RM, Mercer BM, Mansour JM, Redline RW, Moore JJ. 2016. The physiology of fetal membrane weakening and rupture: insights gained from the determination of physical properties revisited. Placenta 42:59–73. https://doi.org/10.1016/j.placenta.2016.03.015.
78. Flores-Pliego A, Espejel-Nunez A, Castillo-Castrejon M, Meraz-Cruz N, Beltran-Montoya J, Zaga-Clavellina V, Nava-Salazar S, Sanchez-Martinez M, Vadillo-Ortega F, Estrada-Gutierrez G. 2015. Matrix metalloproteinase-3 (MMP-3) is an endogenous activator of the MMP-9 secreted by placental leukocytes: implication in human labor. PLoS One 10:e0145366. https://doi.org/10.1371/journal.pone.0145366.
79. Sundrani DP, Chavan-Gautam PM, Pisal HR, Mehendale SS, Joshi SR. 2012. Matrix metalloproteinase-1 and -9 in human placenta during spontaneous vaginal delivery and caesarean sectioning in preterm pregnancy. PLoS One 7:e29855. https://doi.org/10.1371/journal.pone.0029855.
80. Walsh SW, Nugent WH, Solotskaya AV, Anderson CD, Grider JR, Strauss JF, III. 2017. Matrix metalloprotease-1 and elastase are novel uterotonic agents acting through protease-activated receptor 1. Reprod Sci 25:1058–1066. https://doi.org/10.1177/1933719117732162.

81. Tambor V, Kacerovsky M, Lenco J, Bhat G, Menon R. 2013. Proteomics and bioinformatics analysis reveal underlying pathways of infection associated histologic chorioamnionitis in pPROM. Placenta 34:155–161. https://doi.org/10.1016/j.placenta.2012.11.028.
82. Harris LK, Smith SD, Keogh RJ, Jones RL, Baker PN, Knofler M, Cartwright JE, Whitley GS, Aplin JD. 2010. Trophoblast- and vascular smooth muscle cell-derived MMP-12 mediates elastolysis during uterine spiral artery remodeling. Am J Pathol 177:2103–2115. https://doi.org/10.2353/ajpath.2010.100182.
83. Marder W, Knight JS, Kaplan MJ, Somers EC, Zhang X, O'Dell AA, Padmanabhan V, Lieberman RW. 2016. Placental histology and neutrophil extracellular traps in lupus and pre-eclampsia pregnancies. Lupus Sci Med 3:e000134. https://doi.org/10.1136/lupus-2015-000134.
84. Gupta AK, Hasler P, Holzgreve W, Gebhardt S, Hahn S. 2005. Induction of neutrophil extracellular DNA lattices by placental microparticles and IL-8 and their presence in preeclampsia. Hum Immunol 66:1146–1154. https://doi.org/10.1016/j.humimm.2005.11.003.
85. Gomez-Lopez N, Romero R, Leng Y, Garcia-Flores V, Xu Y, Miller D, Hassan SS. 2017. Neutrophil extracellular traps in acute chorioamnionitis: a mechanism of host defense. Am J Reprod Immunol [. https://doi.org/10.1111/aji.12617.
86. Kothary V, Doster RS, Rogers LM, Kirk LA, Boyd KL, Romano-Keeler J, Haley KP, Manning SD, Aronoff DM, Gaddy JA. 2017. Group B Streptococcus induces neutrophil recruitment to gestational tissues and elaboration of extracellular traps and nutritional immunity. Front Cell Infect Microbiol 7:19. https://doi.org/10.3389/fcimb.2017.00019.
87. Boldenow E, Gendrin C, Ngo L, Bierle C, Vornhagen J, Coleman M, Merillat S, Armistead B, Whidbey C, Alishetti V, Santana-Ufret V, Ogle J, Gough M, Srinouanprachanh S, MacDonald JW, Bammler TK, Bansal A, Liggitt HD, Rajagopal L, Adams Waldorf KM. 2016. Group B Streptococcus circumvents neutrophils and neutrophil extracellular traps during amniotic cavity invasion and preterm labor. Sci Immunol 1:eaah4576. https://doi.org/10.1126/sciimmunol.aah4576.
88. Carey AJ, Tan CK, Mirza S, Irving-Rodgers H, Webb RI, Lam A, Ulett GC. 2014. Infection and cellular defense dynamics in a novel 17beta-estradiol murine model of chronic human group B streptococcus genital tract colonization reveal a role for hemolysin in persistence and neutrophil accumulation. J Immunol 192:1718–1731. https://doi.org/10.4049/jimmunol.1202811.
89. Korir ML, Laut C, Rogers LM, Plemmons JA, Aronoff DM, Manning SD. 2016. Differing mechanisms of surviving phagosomal stress among group B Streptococcus strains of varying genotypes. Virulence 8:924–937. https://doi.org/10.1080/21505594.2016.1252016.
90. Manning SD, Lewis MA, Springman AC, Lehotzky E, Whittam TS, Davies HD. 2008. Genotypic diversity and serotype distribution of group B streptococcus isolated from women before and after delivery. Clin Infect Dis 46:1829–1837. https://doi.org/10.1086/588296.
91. Gendrin C, Vornhagen J, Armistead B, Singh P, Whidbey C, Merillat S, Knupp D, Parker R, Rogers LM, Quach P, Iyer LM, Aravind L, Manning SD, Aronoff DM, Rajagopal L. 2018. A nonhemolytic group B Streptococcus strain exhibits hypervirulence. J Infect Dis 217:983–987. https://doi.org/10.1093/infdis/jix646.
92. Manning SD, Springman AC, Lehotzky E, Lewis MA, Whittam TS, Davies HD. 2009. Multilocus sequence types associated with neonatal group B streptococcal sepsis and meningitis in Canada. J Clin Microbiol 47:1143–1148. https://doi.org/10.1128/JCM.01424-08.
93. Iqbal J, Dufendach KR, Wellons JC, Kuba MG, Nickols HH, Gomez-Duarte OG, Wynn JL. 2016. Lethal neonatal meningoencephalitis caused by multi-drug resistant, highly virulent Escherichia coli. Infect Dis (Lond) 48:461–466. https://doi.org/10.3109/23744235.2016.1144142.
94. Schindelin J, Arganda-Carreras I, Frise E, Kaynig V, Longair M, Pietzsch T, Preibisch S, Rueden C, Saalfeld S, Schmid B, Tinevez JY, White DJ, Hartenstein V, Eliceiri K, Tomancak P, Cardona A. 2012. Fiji: an open-source platform for biological-image analysis. Nat Methods 9:676–682. https://doi.org/10.1038/nmeth.2019.
95. McCloy RA, Rogers S, Caldon CE, Lorca T, Castro A, Burgess A. 2014. Partial inhibition of Cdk1 in G 2 phase overrides the SAC and decouples mitotic events. Cell Cycle 13:1400–1412. https://doi.org/10.4161/cc.28401.
96. Doster RS, Kirk LA, Tetz LM, Rogers LM, Aronoff DM, Gaddy JA. 2017. Staphylococcus aureus infection of human gestational membranes induces bacterial biofilm formation and host production of cytokines. J Infect Dis 215:653–657. https://doi.org/10.1093/infdis/jiw300.